

Zeros of the Potts Model Partition Function in the Large- q Limit

Shu-Chiuan Chang^{a,b} Robert Shrock^c

(a) Department of Physics
National Cheng Kung University
Tainan 70101, Taiwan

(b) Physics Division
National Center for Theoretical Science
National Taiwan University
Taipei 10617, Taiwan and

(c) C. N. Yang Institute for Theoretical Physics
State University of New York
Stony Brook, N. Y. 11794

We study the zeros of the q -state Potts model partition function $Z(\Lambda, q, v)$ for large q , where v is the temperature variable and Λ is a section of a regular d -dimensional lattice with coordination number κ_Λ and various boundary conditions. We consider the simultaneous thermodynamic limit and $q \rightarrow \infty$ limit and show that when these limits are taken appropriately, the zeros lie on the unit circle $|x_\Lambda| = 1$ in the complex x_Λ plane, where $x_\Lambda = vq^{-2/\kappa_\Lambda}$. For large finite sections of some lattices we also determine the circular loci near which the zeros lie for large q .

PACS numbers: 05.20.-y, 64.60.Cn, 75.10.Hk

I. INTRODUCTION

In this paper we shall study the q -state Potts model in the limit $q \rightarrow \infty$ and shall present some new results on the complex-temperature zeros of the partition function in this limit. The Potts model has served as a valuable model for the study of phase transitions and critical phenomena [1, 2]. The $q \rightarrow \infty$ limit of the model is exactly solvable on any lattice [3], as can be seen from the fact that in this limit the model essentially reduces to a single-site problem. Since the $q \rightarrow \infty$ limit of the Potts model is solvable, it is natural to investigate the properties of the model for large q . Indeed, although we will focus on partition function zeros rather than physical applications, we note that the Potts model with large q has been used in modelling the kinetic behavior of soap froths [4].

The (zero-field) Potts model is defined, for temperature T on a lattice Λ , or more generally, a graph G , by the partition function

$$Z(G, q, v) = \sum_{\{\sigma_n\}} \exp(K \sum_{\langle ij \rangle} \delta_{\sigma_i, \sigma_j}) \quad (1.1)$$

where $\sigma_i = 1, \dots, q$ are the classical spin variables on each vertex (site) $i \in G$, $\langle ij \rangle$ denotes pairs of adjacent vertices, $K = \beta J$ where $\beta = (k_B T)^{-1}$, and J is the spin-spin coupling. We use the notation $a = e^K$, and $v = a - 1 = e^K - 1$. For the Potts ferromagnet, $J > 0$ so $v \geq 0$, while for the antiferromagnet, $J < 0$ so that $-1 \leq v \leq 0$. The graph G is formally defined by its set of vertices V and its set of edges (= bonds) E ; we denote the number of vertices of G as $n = n(G) = |V|$ and the number of edges of G as $e(G) = |E|$. The complex-temperature zeros of $Z(G, q, v)$, i.e., the zeros in the complex v plane, have the property that on a regular lattice graph with dimensionality greater than the lower critical dimensionality, $d \geq 2$, in the thermodynamic limit $L_j \rightarrow$

∞ with L_j/L_k a finite nonzero constant, $1 \leq j, k \leq d$, they merge to form a locus \mathcal{B} consisting of curves that bound regions of different analytic behavior for the corresponding free energy $F = -k_B T f$, where the dimensionless function f is given by $f = \lim_{n \rightarrow \infty} n^{-1} \ln Z$. For the thermodynamic limit of a graph which is a section of a regular lattice graph Λ with some boundary conditions, we denote κ_Λ as the coordination number satisfying $\kappa_\Lambda = 2 \lim_{n(G) \rightarrow \infty} e(G)/n(G)$ in this limit (independent of boundary conditions). Reviews of the Potts model include [1, 2].

Let $G' = (V, E')$ be a spanning subgraph of G , i.e. a subgraph having the same vertex set V and a subset of the edge set, $E' \subseteq E$. Then a useful representation of $Z(G, q, v)$ is [5]

$$Z(G, q, v) = \sum_{G' \subseteq G} q^{k(G')} v^{e(G')} \quad (1.2)$$

where $k(G')$ denotes the number of connected components of G' . Since we only consider connected lattice graphs G , we have $k(G) = 1$. For the ferromagnet, eq. (1.2) allows one to generalize q from the positive integers to the positive reals, \mathbb{R}_+ . As is evident from eq. (1.2), $Z(G, q, v)$ is a polynomial in q with minimal and maximal degrees 1 and $n(G)$, and a polynomial in v with minimal and maximal degrees 0 and $e(G)$. Thus, for a finite G , $Z(G, q, v)$ is completely determined by its zeros and can be written as $Z(G, q, v) = \prod_{i=1}^{e(G)} [v - v_i(q)]$.

We first recall some previous related work. For the special case $q = 2$ on the square lattice, where one has the exact Onsager solution for the partition function, it was found that (in the thermodynamic limit) the locus \mathcal{B} consists of the union of circles $|a \pm 1| = \sqrt{2}$ [6]. The locus \mathcal{B} has also been determined exactly for $q = 2$ on various other $d = 2$ lattices (e.g., [7, 8]). However, aside from the special case $q = 2, d = 2$, one does not, in general,

know \mathcal{B} for lattice graphs of dimensionality $d \geq 2$. Indeed, studies of complex-temperature zeros of the Potts model partition function for finite sections of various lattices have found that they exhibit a considerable scatter, especially in the half-plane with $Re(a) < 0$ [9]-[17]. A complementary approach has been to obtain exact solutions for the partition function and finite-width strips of lattices with various boundary conditions and hence determine exactly the locus \mathcal{B} in the infinite-length limit (e.g., [18]-[23]). These systems are quasi-one-dimensional, so that \mathcal{B} does not cross the positive real a axis, i.e., the free energy is analytic for all nonzero temperatures. With the definition $x_{sq} = v/\sqrt{q}$ for the square lattice, it was found the complex-temperature zeros calculated for finite sections of this square lattice with duality-preserving boundary conditions have the property that a subset lies exactly on an arc of the unit circle $|x_{sq}| = 1$ in the complex x_{sq} plane for $Re(x_{sq}) \gtrsim 0$ [10, 11, 12, 22]. For physical temperature the coefficients of powers of $a = e^K$ are positive, so there are no zeros on the positive real axis $Re(a) > 0$ for any finite lattice. However, in the thermodynamic limit, the phase boundary on \mathcal{B} crosses this axis at the ferromagnetic phase transition point, $a_c = 1 + \sqrt{q}$, i.e. $x_c = 1$. A number of interesting results have been obtained by F. Y. Wu and collaborators: in Ref. [11] a conjecture was made that for finite sections of the square lattice with self-dual boundary conditions and for the same lattice with free or periodic boundary conditions in the thermodynamic limit, the complex-temperature zeros of the partition function in the $Re(x_{sq}) > 0$ half-plane are located on the unit circle $|x_{sq}| = 1$. In Ref. [12], it was shown, using Euler's identity for integer partitions, that for the Potts model on the self-dual square lattice, if one takes the limit $q \rightarrow \infty$, all of the zeros of the partition function are located on this unit circle $|x_{sq}| = 1$ for any lattice size. In Refs. [12, 24, 25] it was shown that partition function for the Potts model on a finite d -dimensional Cartesian lattice \mathbb{E}^d with $d \geq 2$ and appropriate boundary conditions, in the limit $q \rightarrow \infty$, divided by an appropriate power of q , is given by the generating function of restricted integer partitions in $d - 1$ dimensions, with expansion variable $t = v^d/q$.

In the present paper we present some results on the zeros of the Potts model partition function for large q on general regular d -dimensional lattices, both in the thermodynamic limit and for finite lattices, with various boundary conditions. We shall give a simple proof for an arbitrary regular lattice of dimension $d \geq 2$ that, when the thermodynamic limit and the $q \rightarrow \infty$ limit are taken in an appropriate way, the zeros of the partition function lie on the circle $|x_\Lambda| = 1$. This generalizes the corresponding result of Wu and coworkers from a Cartesian lattice \mathbb{E}^d to an arbitrary regular d -dimensional lattice. We also consider finite sections of some regular lattices and determine the circular loci near which the zeros lie for large q . We shall often call this the "approximating circle" for the zeros.

II. GENERAL RESULTS FOR LARGE q

In this section we analyze the pattern of partition function zeros of the Potts model for large q . Let us first arrange the terms in eq. (1.2) in order of decreasing power of v , from $v^{e(G)}$ to 1. There are $\binom{e(G)}{j}$ terms in the coefficients of $v^{e(G)-j}$ and v^j , so that in the special case $q = 1$ the partition function reduces to $Z(G, q = 1, v) = (v + 1)^{e(G)}$. These $\binom{e(G)}{j}$ terms can have different powers in q except for very small or very large j , as follows. The term with the highest power of v arises from the contribution of $G' = G$ in eq. (1.2), where all of the edges of G are present, and the power of v is $e(G)$; since this graph consists of a single connected component, the coefficient is q and the term is $qv^{e(G)}$. In considering other terms in $Z(G, q, v)$, we assume that the graph G has the property that the removal of a few edges does not cut it into disconnected components. This excludes the cases of a one-dimensional lattice and quasi-one-dimensional lattice strips of narrow widths; we comment on these in the appendix. For example, for a regular d -dimensional lattice graph, we require that $d \geq 2$ and that the lengths L_k with $1 \leq k \leq d$ are great enough so that this condition is satisfied. Next, the term in $Z(G, q, v)$ with one lower power of v is obtained from the set of G' each of which has an edge set E' with one less edge than the full edge set E . This term is $\binom{e(G)}{1} q v^{e(G)-1}$, where $\binom{\ell}{m} = \ell!/[m!(\ell - m)!]$. Similarly, the first few terms with descending powers of v below the maximal power are given by $\binom{e(G)}{j} q v^{e(G)-j}$, where j edges are removed in G' and the linear dependence on q reflects the property that this edge removal maintains the connectedness of the resulting G' , so $k(G') = 1$. In general, this holds for $j < \delta(G)$, where $\delta(G)$ and $\Delta(G)$ denote the minimal and maximal degrees of a vertex in G . (The degree of a vertex is defined as the number of edges connected to it). Thus, for example, a term involving q^2 begins to appear in the coefficient of $v^{e(G)-3}$ for cyclic strips of the square lattice with $L_1 \equiv L_x > 2$ and $L_2 \equiv L_y \geq 2$ since the degree of vertices on the upper and lower boundaries is three, but it appears in the coefficient of $v^{e(G)-2}$ for the same strip with $L_x = 2$. At the other end of the polynomial $Z(G, q, v)$ ordered as powers of v , the term with the power of v equal to zero arises from the contribution of G' with $E' = \emptyset$, i.e., the spanning subgraph containing no edges, leaving the $n(G)$ vertices as disconnected components; this term is thus $q^{n(G)}$. The term linear in v results from the contributions of spanning subgraphs G' with one edge and is $e(G) q^{n(G)-1} v$. In general, the first few such terms are given by $\binom{e(G)}{j} q^{n(G)-j} v^j$, where G' consist of j edges such that $j < g(G)$, with $g(G)$ denoting the girth of G , i.e., the length of minimum closed circuit on G . For example, for cyclic strips of the square lattice again, the term $q^{n(G)-3}$ appears first in the coefficient of v^4 for $L_x > 3$ because the girth is four, but term $q^{n(G)-2}$ appears first in the coefficient of v^3 if $L_x = 3$ and the term

$q^{n(G)-1}$ appears in the coefficient of v^2 if $L_x = 2$. Thus, for graphs G satisfying the above-mentioned conditions, we have

$$\begin{aligned} Z(G, q, v) &= \sum_{j=0}^{e(G)} c_j(q) v^j \\ &= qv^{e(G)} + e(G)qv^{e(G)-1} + \binom{e(G)}{2}qv^{e(G)-2} + \dots \\ &+ \binom{e(G)}{2}q^{n(G)-2}v^2 + e(G)q^{n(G)-1}v + q^{n(G)} \end{aligned} \quad (2.1)$$

where the coefficients $c_j(q)$ are polynomials in q .

Now let us consider the limit $q \rightarrow \infty$. Evidently, in this limit, for a given finite graph G , there is a single dominant term in $Z(G, q, v)$, namely q^n , arising from G' with $E' = \emptyset$. This term is what one would get in the evaluation of Z if there were no spin-spin interactions, but instead just single-site contributions. This reduction helps to understand the fact that the Potts model is exactly solvable [3] in the limit $q \rightarrow \infty$.

Next, let us examine the terms in $Z(G, q, v)$ in more detail. For a given graph G , we define

$$x_G = \frac{v}{q^{n(G)/e(G)}} \quad (2.2)$$

and, in the thermodynamic limit,

$$x_\Lambda = \frac{v}{q^{2/\kappa_\Lambda}}. \quad (2.3)$$

Considering q to be large, we focus on the first two and last two of the terms in eq. (2.1); we can write these as

$$\begin{aligned} Z(G, q, v) &= q^{n(G)+1} \left[x_G^{e(G)} \{1 + e(G)[x_G q^{n(G)/e(G)}]^{-1}\} + \dots \right. \\ &+ \left. q^{-1} \{e(G) x_G q^{(n(G)/e(G)-1)} + 1\} \right]. \end{aligned} \quad (2.4)$$

We can approximate $Z(G, q, v)$ by including just the first and last terms if several conditions are met. In the expression multiplying $x_G^{e(G)}$, the second term is negligible compared with the first if $x_G \sim O(1)$ and the condition

$$q \gg e(G)^{e(G)/(n(G)-1)} \quad (2.5)$$

is satisfied. In the expression multiplying q^{-1} , the first term is negligible compared with the second if $x_G \sim O(1)$ and the condition

$$q \gg [e(G)]^{e(G)/(e(G)-n(G)+1)} \quad (2.6)$$

is satisfied. Let us denote the degree of $c_j(q)$ in q as p_j . Among the $\binom{e(G)}{j}$ terms in $c_j(q)$, only a few have this power except for small and large j as discussed above.

Now we require that $c_j(q)v^j$ be small compared with q^n , so that in terms of the power of q ,

$$p_j + j \left(\frac{n(G)-1}{e(G)} \right) < n(G) \quad (2.7)$$

or

$$p_j < \frac{(e(G)-j)(n(G)-1)}{e(G)} + 1. \quad (2.8)$$

Further, if these conditions hold and $x_G \sim O(1)$, then terms arising from the third, fourth, and subsequent terms of $Z(G, q, v)$ are small relative to the first, and the third, fourth, and earlier terms counting in from the last, are negligible relative to the last, with the ordering specified by ascending powers of v , as in eq. (2.1). Provided that $x_G \sim O(1)$ and the above conditions hold, one can approximate $Z(G, q, v)$ by keeping only the first and last terms in eq. (2.1):

$$Z(G, q, v) \sim qv^{e(G)} + q^{n(G)} = q^{n(G)+1} [x_G^{e(G)} + q^{-1}]. \quad (2.9)$$

The zeros of this approximation to $Z(G, q, v)$ are given by

$$x_G = (-q^{-1})^{1/e(G)}. \quad (2.10)$$

Now consider the limit $e(G) \rightarrow \infty$ and $n(G) \rightarrow \infty$ with the ratio $e(G)/n(G) = \kappa_G/2$ finite. If q also goes to infinity, sufficiently fast to satisfy the conditions (2.5) and (2.6) but more slowly than the exponential $e^{be(G)}$ with b a real positive constant, then

$$\lim_{q \rightarrow \infty} \lim_{e(G) \rightarrow \infty} |q|^{1/e(G)} = 1, \quad (2.11)$$

and these zeros merge onto the unit circle

$$|x_G| = 1. \quad (2.12)$$

If q were to grow more rapidly, as $q \sim e^{be(G)}$ where b is an arbitrary positive real constant, then the zeros would merge onto the circle $|x_G| = e^{-b}$.

In particular, one may consider the thermodynamic limit of a graph G which is a section of the regular lattice Λ . Then the conditions corresponding to eqs. (2.5) and (2.6) are, respectively,

$$q \gg e(G)^{\kappa_\Lambda/2} \quad (2.13)$$

and

$$q \gg e(G)^{\kappa_\Lambda/(\kappa_\Lambda-2)}. \quad (2.14)$$

The inequality $\kappa_\Lambda/2 \geq \kappa_\Lambda/(\kappa_\Lambda-2)$ is equivalent to the inequality $\kappa_\Lambda \geq 4$. Since $\kappa_\Lambda \geq 4$ for all of the lattices that we consider except for the honeycomb lattice, a consequence is that for these former lattices with $\kappa_\Lambda \geq 4$, condition (2.13) implies condition (2.14). Provided that $x_\Lambda \sim O(1)$ and the above conditions hold, so that one can approximate $Z(G, q, v)$ with the first and last terms

in eq. (2.1), it follows that in this thermodynamic limit, with q also going to infinity sufficiently fast to satisfy the conditions (2.13) and (2.14) but more slowly than the exponential form given above, the zeros of $Z(G, q, v)$ merge onto the circle

$$|x_\Lambda| = 1 \quad (2.15)$$

where x_Λ is given by eq. (2.3). Our result (2.15) holds for any regular lattice with dimension $d \geq 2$. For example, for the d -dimensional Cartesian lattice \mathbb{E}^d , $\kappa_{\mathbb{E}^d} = 2d$, while for the d -dimensional body-centered cubic lattice, $\kappa_{bcc^d} = 2^d$.

Since the free energy is nonanalytic at $x_\Lambda = 1$, eq. (2.15) yields the asymptotic relations

$$v_{c,\Lambda} \sim q^{2/\kappa_\Lambda} \quad \text{as } q \rightarrow \infty \quad (2.16)$$

and hence

$$K_{c,\Lambda} \sim \frac{2}{\kappa_\Lambda} \ln q \quad \text{as } q \rightarrow \infty \quad (2.17)$$

for the values of v and K where the Potts model on the lattice Λ has a phase transition from a paramagnetic (PM) high-temperature phase to a ferromagnetic (FM) low-temperature phase in the limit of large q . We note that this agrees with the large- q limit of the mean-field theory result [26]

$$K_{c,MFT} = \frac{2(q-1)}{\kappa_\Lambda(q-2)} \ln(q-1), \quad (2.18)$$

viz.,

$$K_{c,MFT} \sim \frac{2}{\kappa_\Lambda} \left[\{1 + q^{-1} + O(q^{-2})\} \ln q - \{q^{-1} + O(q^{-2})\} \right] \quad (2.19)$$

as $q \rightarrow \infty$. In eqs. (2.17) and (2.18), the property that K_c increases with increasing q can be understood as a consequence of the fact that as q gets large, each spin has more possible values (is “floppier”), and hence one must go to a lower temperature for the ferromagnetic long-range order to occur. The feature that K_c increases asymptotically like $\ln q$ as $q \rightarrow \infty$ can be understood since an order-disorder transition involves a balance between minimizing the configurational energy and maximizing the entropy terms in the free energy per site, $F = U - TS$, and in this limit, the entropy per site is $S \rightarrow k_B \ln q$.

Next, we recall the known exact equations for the PM-FM phase transition on the 2D lattices [1, 2], which we write in a convenient manner for the discussion of the large- q limit,

$$\begin{aligned} \frac{q}{v^2} &= 1 & \text{for } \Lambda = sq \\ \frac{q}{v^3} &= 1 + \frac{3}{v} & \text{for } \Lambda = tri \end{aligned}$$

$$\frac{q^2}{v^3} = 1 - \frac{3q}{v^2} \quad \text{for } \Lambda = hc, \quad (2.20)$$

where sq , tri , and hc denote the square, triangular, and honeycomb lattices. As is evident, in the limit of large q and v such that $q = v^2$ for the square lattice, $q = v^3$ for the triangular lattice and $q = v^{3/2}$ for the honeycomb lattice, these equations are all in agreement with the general relation (2.16), which also holds for higher-dimensional lattices.

III. PARTITION FUNCTION ZEROS FOR FINITE LATTICE SECTIONS

A. General Structure

It is also of interest to consider zeros of $Z(G, q, v)$ on finite lattice graphs in the limit of large q . In general, if the conditions specified in the previous section are satisfied, one can approximate $Z(G, q, v)$ by keeping the first and last terms in eq. (2.1). We have studied these zeros in detail for sections of various 2D lattices and have found that a sufficient criterion that these conditions can be satisfied for these and higher-dimensional lattices is that one uses fully periodic boundary conditions. Accordingly, when q is large, the zeros in the x_Λ plane are located close to a circle. For finite lattice graphs with fully periodic boundary conditions, $e(G)/n(G) = \kappa_\Lambda/2$ so that the two definitions in eqs.(2.2) and (2.3) are equivalent. However, for finite graphs with other boundary conditions, x_G varies from one graph to another. Therefore, we will plot zeros in the x_Λ plane for the lattice Λ with different boundary conditions. We first rewrite the approximate expression (2.9) in an equivalent form that will be convenient for our discussion; when q is large,

$$\begin{aligned} Z(G, q, v) &\sim qv^{e(G)} + q^{n(G)} \\ &= q^{(2e(G)/\kappa_\Lambda)+1} [x_\Lambda^{e(G)} + q^{n(G)-(2e(G)/\kappa_\Lambda)-1}] \end{aligned} \quad (3.1)$$

The zeros of this approximation to $Z(G, q, v)$ are located on a circle in the x_Λ plane with radius

$$r(\Lambda, BC) = q^{p(\Lambda, BC)} \quad (3.2)$$

where

$$p(\Lambda, BC) = \frac{n(G)-1}{e(G)} - \frac{2}{\kappa_\Lambda}. \quad (3.3)$$

(This power p should not be confused with the powers p_j in eqs. (2.7), (2.8). The radius $r(\Lambda, BC)$ is less (greater) than unity if $p(\Lambda, BC)$ is negative (positive). For lattices with periodic boundary conditions in all directions, $n(G)/e(G) = 2/\kappa_\Lambda$ and hence

$$p(\Lambda, PBC) = -\frac{1}{e(G)} \quad (3.4)$$

as in eq. (2.10).

In our explicit calculations of zeros for various lattices, we have found that for large but finite q , the approximating circles near which these zeros lie may have centers that are slightly shifted to the left or right of the origin of the x_Λ plane and move in toward the origin as $q \rightarrow \infty$. The following analysis provides an understanding of these shifts. As discussed in Section II, there are $\delta(G)$ terms in the partition function given by $\binom{e(G)}{j} q v^{e(G)-j}$ and there are $g(G)$ terms given by $\binom{e(G)}{j} q^{n(G)-j} v^j$. For the finite lattice graphs with large vertex degree and small girth, a specific approximation for the partition function $Z(G, q, v)$ when q is large is

$$Z(G, q, v) \sim q(v+1)^{e(G)} + q^{n(G)} \quad (3.5)$$

so that the center of the circle, denoted by $c(\Lambda, BC)$, is not at the origin but at

$$c(\Lambda, BC) = -\frac{1}{q^{2/\kappa_\Lambda}}. \quad (3.6)$$

Of course, this approaches zero as $q \rightarrow \infty$, in agreement with our result above, eq. (2.15). The triangular lattice is an example for which the center of the circle is shifted to the left, as in eq. (3.6) and will be discussed below.

On the other hand, for finite lattice graphs with small vertex degree and large girth, a specific approximation for $Z(G, q, v)$ when q is large is

$$\begin{aligned} Z(G, q, v) &\sim qv^{e(G)} + q^{n(G)-e(G)}(q+v)^{e(G)} \\ &= q^{n(G)+1} [x_G^{e(G)} + q^{-1}(1 + q^{n(G)/e(G)-1} x_G)^{e(G)}] \end{aligned} \quad (3.7)$$

The circle near which the zeros lie is now shifted to the right. Let us first consider the case with fully periodic boundary conditions so that $x_G = x_\Lambda$. In the complex x_Λ plane, the circle has radius

$$r(\Lambda, PBC) = \frac{q^{1/e(G)}}{q^{2/e(G)} - q^{(2n(G)/e(G))-2}} \quad (3.8)$$

and center at

$$c(\Lambda, PBC) = \frac{q^{n/e(G)-1}}{q^{2/e(G)} - q^{(2n(G)/e(G))-2}}. \quad (3.9)$$

For the lattices with $e(G)$ larger than $n(G)$, the term $q^{(2n(G)/e(G))-2}$ in the denominator is negligible when q is large, and the radius of the circle is approximately $q^{-1/e(G)}$, as in eq. (3.2). For large q , the center of the circle in the x_Λ plane is

$$c(\Lambda, PBC) = q^{-s(\Lambda, BC)} \quad (3.10)$$

where

$$s(\Lambda, PBC) = 1 + \frac{2 - n(G)}{e(G)}. \quad (3.11)$$

When $e(G)$ is large, so that $2/e(G) \ll 1$, the position of center can be further approximated as $c(\Lambda, PBC) \simeq q^{(2/\kappa_\Lambda)-1}$, which approaches the origin as $q \rightarrow \infty$.

For the lattice sections with other boundary conditions, a specific approximation for $Z(G, q, v)$ for large q is

$$\begin{aligned} Z(G, q, v) &\sim q^{(2e(G)/\kappa_\Lambda)+1} \times \\ &[x_\Lambda^{e(G)} + q^{n(G)-(2e(G)/\kappa_\Lambda)-1} (1 + q^{(2/\kappa_\Lambda)-1} x_\Lambda)^{e(G)}] \end{aligned} \quad (3.12)$$

In the x_Λ plane, the resultant approximating circle has radius

$$r(\Lambda, BC) = \frac{q^{1/e(G)-(n(G)/e(G))+2/\kappa_\Lambda}}{q^{2/e(G)-(2n(G)/e(G))+4/\kappa_\Lambda} - q^{(4/\kappa_\Lambda)-2}} \quad (3.13)$$

and center

$$c(\Lambda, BC) = \frac{q^{(2/\kappa_\Lambda)-1}}{q^{2/e(G)-(2n(G)/e(G))+4/\kappa_\Lambda} - q^{(4/\kappa_\Lambda)-2}}. \quad (3.14)$$

For lattices with $\kappa_\Lambda > 2$, $q^{4/\kappa_\Lambda-2}$ in the denominator is negligible when q is large, and the radius of the circle is the same as eqs. (3.2) and (3.3). We also have

$$s(\Lambda, BC) = 1 + \frac{2 - 2n(G)}{e(G)} + \frac{2}{\kappa_\Lambda} \quad (3.15)$$

for large q . The honeycomb lattice is an example for which the circle near which the zeros lie shifts to the right of the origin and will be discussed below. Another example is the square lattice with next-nearest-neighbor interactions that have the same strength as the nearest-neighbor interactions, which we have also analyzed. From the above discussion, we expect that the center of the circle is the origin for lattice sections with vertex degree roughly equal to girth.

B. Square Lattice Sections

For the square lattice with toroidal (tor) boundary conditions, $e(sq, tor) = 2L_x L_y$, $\kappa_{sq} = 4$, and

$$p(sq, tor) = -\frac{1}{2L_x L_y}. \quad (3.16)$$

Hence the radius of the approximating circle increases as the area of the lattice increases, and approaches unity from below in the thermodynamic limit. The zeros of the partition function for the Potts model on the toroidal strip of the square lattice with $L_y = 4$ and $L_x = 9$ in the x_{sq} plane when $q = 1000$ are shown in Fig. 1(a). The radius of the circle is about 0.9085. The zeros lie very close to this circle for the above value of q , and we find that they get closer to the circle given by eqs. (3.2) and (3.3) when q increases.

For the square lattice with cyclic boundary conditions we have $e(sq, cyc) = L_x(2L_y - 1)$. By eq.(3.3),

$$p(sq, cyc) = \frac{L_x - 2}{2L_x(2L_y - 1)}. \quad (3.17)$$

In the thermodynamic limit the radius of the approximating circle decreases and approaches unity from above. Note that if one were to keep L_y fixed and take $L_x \rightarrow \infty$, thereby violating the premises of our analysis, the radius of this approximating circle would be $q^{1/2(2L_y-1)}$, which would diverge as $q \rightarrow \infty$. The zeros of the cyclic strip with $L_y = 4$ and $L_x = 9$ in the x_{sq} plane when $q = 1000$ are shown in Fig. 1(b). The radius of the approximating circle is about 1.47. The zeros are not as close to the circle as for the corresponding toroidal case. On the other hand, if one keeps L_x fixed and takes $L_y \rightarrow \infty$, corresponding to cylindrical boundary conditions, the radius of the approximating circle approaches unity from above. The zeros of the cylindrical strip with $L_y = 4$ and $L_x = 9$ in the x_{sq} plane when $q = 1000$ are shown in Fig. 1(c). The radius of this approximating circle is about 1.11. The zeros are closer to the circle than the cyclic strip with the same L_y and L_x because the number of boundary vertices (i.e. vertices with coordination number three) is reduced.

For the square lattice with free boundary conditions, $e(sq, free) = 2L_xL_y - L_x - L_y$. By eq.(3.3),

$$p(sq, free) = \frac{L_x + L_y - 2}{2(2L_xL_y - L_x - L_y)}. \quad (3.18)$$

In the thermodynamic limit the radius of the circle decreases and approaches unity from above. Again, however, if one were to keep L_y fixed and take $L_x \rightarrow \infty$, the radius of the approximating circle would be $q^{1/2(2L_y-1)}$, (the same as the cyclic case), which would diverge as $q \rightarrow \infty$. Since for a given lattice size the number of boundary vertices is larger than for other boundary conditions, and especially since there are four vertices with coordination number equal to two, it is natural to expect that the zeros will lie farther from the asymptotic circle than for these other boundary conditions. The zeros of the free strip with $L_y = 4$ and $L_x = 9$ in the x_{sq} plane when $q = 1000$ are shown in Fig. 1(d). The radius of the approximating circle is about 1.90.

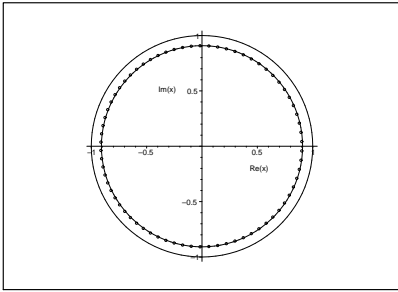
C. Triangular lattice

For the triangular lattice with toroidal boundary conditions, $e(tri, tor) = 3L_xL_y$ and $\kappa(tri, tor) = 6$. Hence, for a finite section of the triangular lattice with toroidal boundary conditions, as for the infinite triangular lattice,

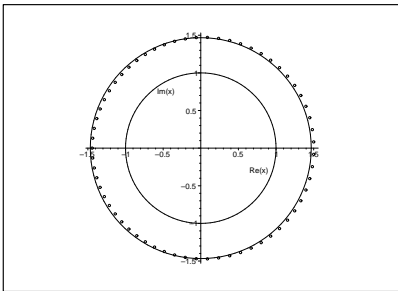
$$x_{tri} = \frac{v}{q^{1/3}} \quad (3.19)$$

and

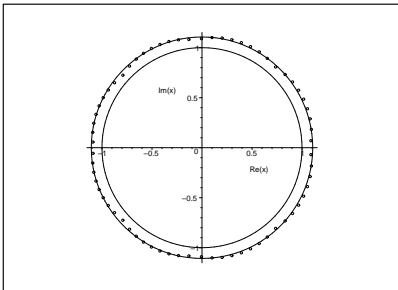
$$p(tri, tor) = -\frac{1}{3L_xL_y}, \quad (3.20)$$



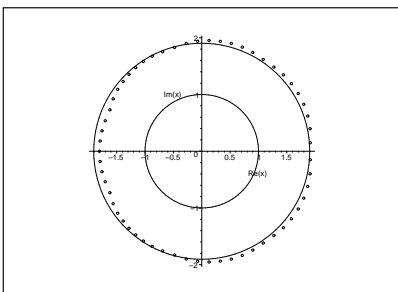
(a)



(b)



(c)



(d)

FIG. 1: Zeros of the Potts model partition function, plotted in the x_{sq} plane, for a section of the square lattice with $L_y = 4$ and $L_x = 9$, when $q = 1000$, for the following boundary conditions: (a) toroidal; (b) cyclic; (c) cylindrical; (d) free. For comparison, the unit circle and circles where the zeros cluster are also shown.

as given by eq.(2.10). This radius increases as the size of the lattice increases, and approaches unity from below in the thermodynamic limit. There is a noticeable shift of the circle to the left. The center of the approximating circle is at $x_{tri} = -q^{-1/3}$, approaching zero as $q \rightarrow \infty$. The zeros of the toroidal strip with $L_y = 3$ and $L_x = 9$ in the x_{tri} plane when $q = 1000$ are shown in Fig. 2(a). The radius of this approximating circle is about 0.918.

For a section of the triangular lattice with cyclic boundary conditions, $e(tri, cyc) = L_x(3L_y - 2)$. When q is large, we calculate

$$p(tri, cyc) = \frac{2L_x - 3}{3L_x(3L_y - 2)} \quad (3.21)$$

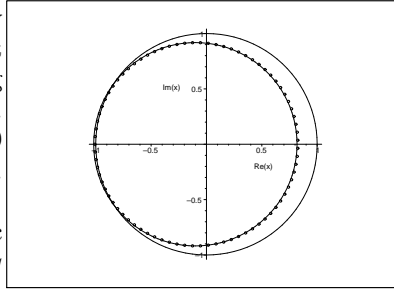
for the approximating circle. In the thermodynamic limit, the radius of this circle decreases, approaching unity from above. However, if one were to keep L_y fixed and take $L_x \rightarrow \infty$, then the radius would be $q^{2/3(3L_y-2)}$, which would diverge as $q \rightarrow \infty$. The zeros of the cyclic strip with $L_y = 4$ and $L_x = 9$ in the x_{tri} plane when $q = 1000$ are shown in Fig. 2(b). The radius of this approximating circle is about 1.47 as for the corresponding case of the square lattice. If one keeps L_x fixed and takes $L_y \rightarrow \infty$, corresponding to cylindrical boundary conditions, the radius of the approximating circle approaches unity from above. The zeros of the cylindrical strip with $L_y = 4$ and $L_x = 9$ in the x_{tri} plane when $q = 1000$ are shown in Fig. 2(c). The radius of this approximating circle is about 1.12.

In general, the approximation in eq.(2.9) is not valid for the triangular lattice with free boundary conditions. The reason is that there are two vertices with degree two, so that the coefficient of $v^{e(tri, free)-2}$ contains the term $2q^2$ and the coefficient of $v^{e(tri, free)-4}$ contains the term q^3 for $L_x, L_y > 2$. Therefore, when q is large there are two pair of roots around $v \sim \pm i\sqrt{q}$, or equivalently around $\pm iq^{1/6}$ in the x_{tri} plane. We have $e(tri, free) = 3L_xL_y - 2L_x - 2L_y + 1$. The partition function zeros for the free strip of the triangular lattice with $L_y = 4$ and $L_x = 9$ when $q = 1000$ are shown in Fig. 2(d). Although the approximation (2.9) does not apply here, one can see that many of these zeros lie close to an approximating circle with radius 1.84, which is similar to what one would get by formally using $p(tri, free) = 2(L_x + L_y - 2)/[3(3L_xL_y - 2L_x - 2L_y + 1)]$. We observe that there are two almost overlapping complex-conjugate pairs of zeros which have relatively large magnitude and are close to the imaginary axis.

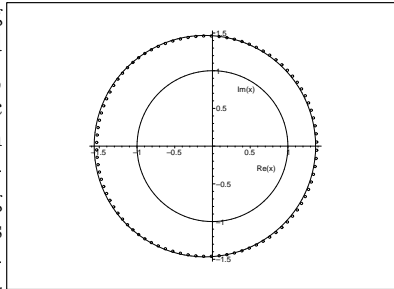
D. Honeycomb lattice

For the honeycomb lattice with toroidal boundary conditions where both L_x and L_y are even, $e(hc, tor) = 3L_xL_y/2$ so that $n(hc, tor)/e(hc, tor) = 2/3$ for any L_x and L_y . Thus,

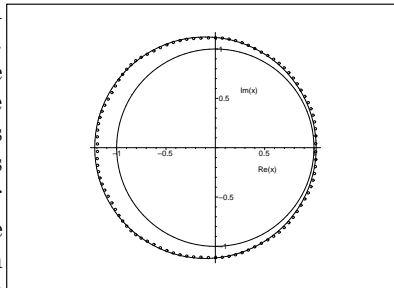
$$x_{hc} = \frac{v}{q^{2/3}} \quad (3.22)$$



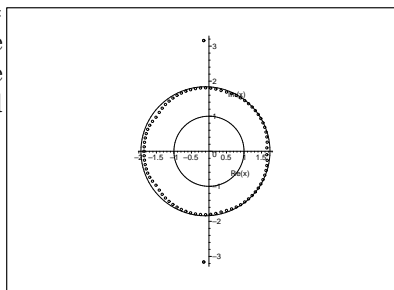
(a)



(b)



(c)



(d)

FIG. 2: Zeros of the Potts model partition function in the x_{tri} plane for the triangular lattice when $q = 1000$, for the following boundary conditions and sizes: (a) toroidal with $L_y = 3$ and $L_x = 9$; (b) cyclic with $L_y = 4$ and $L_x = 9$; (c) cylindrical with $L_y = 4$ and $L_x = 9$; (d) free with $L_y = 4$ and $L_x = 9$. For comparison, the unit circle and approximating circles are also shown.

and

$$p(hc, tor) = -\frac{2}{3L_x L_y}, \quad (3.23)$$

as given in eq.(2.10). This radius increases as the size of the lattice increases, and approaches unity from below in the thermodynamic limit. There is a shift of the circle to the right. By eq.(3.11),

$$s(hc, tor) = \frac{1}{3} + \frac{4}{3L_x L_y} \quad (3.24)$$

which approaches $1/3$ as the size of the lattice section becomes large. The zeros of the toroidal strip with $L_y = 4$ and $m = 9(L_x = 18)$ in the x_{hc} plane when $q = 1000$ are shown in Fig. 3(a). The radius of this approximating circle is about 0.938.

For a section of the honeycomb lattice with cyclic boundary conditions we have $e(hc, cyc) = L_x(3L_y - 1)/2$, where L_x must be even. By eq.(3.3),

$$p(hc, cyc) = \frac{2(L_x - 3)}{3L_x(3L_y - 1)}. \quad (3.25)$$

In the thermodynamic limit, the radius of the approximating circle decreases, approaching unity from above. For the shift of the circle, by eq. (3.15),

$$s(hc, cyc) = \frac{1}{3} + \frac{4(3 - L_x)}{3L_x(3L_y - 1)} \quad (3.26)$$

The zeros of the cyclic strip with $L_y = 4$ and $m = 9(L_x = 18)$ in the x_{hc} plane when $q = 1000$ are shown in Fig. 3(b). The radius of this approximating circle is about 1.42.

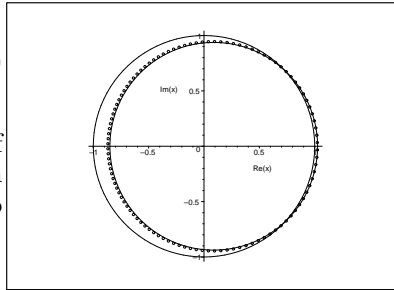
Since we represent the honeycomb lattice in the form of bricks oriented horizontally, the results for cylindrical boundary conditions cannot be obtained from cyclic boundary conditions by simply switching L_x and L_y . We have $e(hc, cyl) = L_y(3L_x/2 - 1)$ for the honeycomb lattice with cylindrical boundary conditions where L_y must be even. When q is large, we calculate

$$p(hc, cyl) = \frac{2(2L_y - 3)}{3L_y(3L_x - 2)}. \quad (3.27)$$

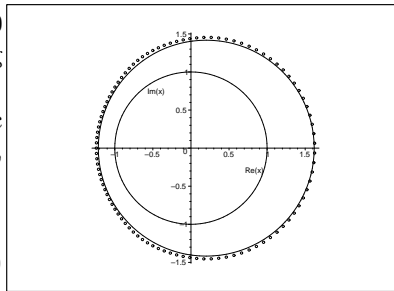
and

$$s(hc, cyl) = \frac{1}{3} + \frac{4(3 - 2L_y)}{L_y(3L_x - 2)}. \quad (3.28)$$

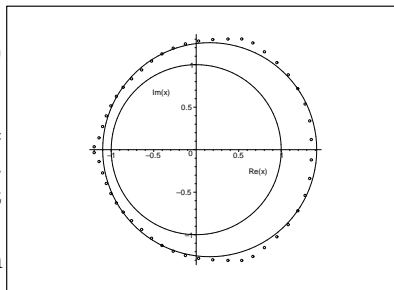
The zeros of the cylindrical strip with $L_y = 4$ and $L_x = 9$ in the x_{hc} plane when $q = 1000$ are shown in Fig. 3(c). The radius of this approximating circle is about 1.26. We have also considered other boundary conditions, as shown in Fig. 3.



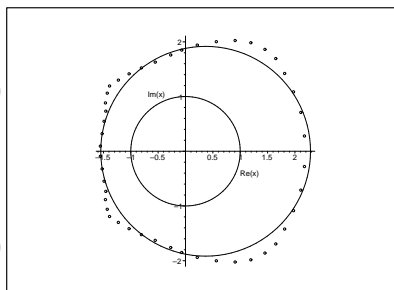
(a)



(b)



(c)



(d)

FIG. 3: Zeros of the Potts model partition function in the x_{hc} plane for the honeycomb lattice when $q = 1000$, for the following boundary conditions and sizes: (a) toroidal with $L_y = 4$ and $L_x = 18$; (b) cyclic with $L_y = 4$ and $L_x = 18$; (c) cylindrical with $L_y = 4$ and $L_x = 9$; (d) free boundary conditions with $L_y = 4$ and $L_x = 9$. For comparison, the unit circle and approximating circles are also shown.

E. Kagomé lattice

As an example of a heteropolygonal two-dimensional lattice (an Archimedean lattice comprised of more than one type of regular polygon), we consider the kagomé lattice. For a section of this lattice with toroidal boundary conditions, $n(kag, tor) = 3L_xL_y$ and $e(kag, tor) = 6L_xL_y$ so that $n(kag, tor)/e(kag, tor) = 1/2$ as for the square lattice. Hence,

$$x_{kag} = \frac{v}{\sqrt{q}} \quad (3.29)$$

and

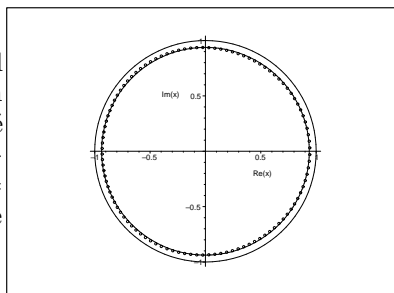
$$p(kag, tor) = -\frac{1}{6L_xL_y}. \quad (3.30)$$

The radius of the approximating circle increases as the size of the lattice increases and approaches unity from below in the thermodynamic limit. The zeros of the toroidal strip with $L_y = 2$ and $L_x = 9$ in the x_{kag} plane when $q = 1000$ are shown in Fig. 4(a). The radius of this approximating circle is about 0.938. We have also considered other boundary conditions as shown in Fig. 4.

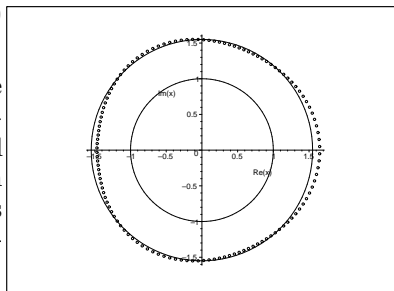
IV. SUMMARY

In summary, we have presented some new results on the distribution of complex-temperature zeros of the partition function of the q -state Potts model for $q \rightarrow \infty$. Generalizing previous work of Wu and coworkers for Cartesian lattices, we have shown that with an appropriate definition of the thermodynamic limit and the limit $q \rightarrow \infty$ on an arbitrary regular lattice Λ of dimensionality $d \geq 2$, the zeros lie on the circle $|x_\Lambda| = 1$. We have also studied the distribution of zeros for finite sections of various two-dimensional lattices for large q , showing how they also lie approximately on circles.

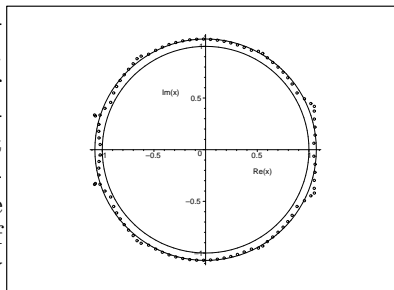
Acknowledgments: The research of R.S. was partially supported by the NSF grant PHY-00-98527. The research of S.C.C. was partially supported by the NSC grant NSC-93-2119-M-006-009, NSC-94-2112-M-006-013 and NSC-94-2119-M-002-001.



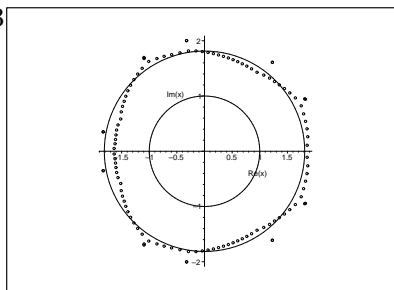
(a)



(b)



(c)



(d)

FIG. 4: Zeros in the x_{kag} plane for Potts model partition function on the Kagomé lattice when $q = 1000$, for the following boundary conditions and sizes: (a) toroidal with $L_y = 2$ and $L_x = 9$; (b) cyclic with $L_y = 3$ and $L_x = 9$; (c) cylindrical with $L_y = 2$ and $L_x = 9$; (d) free with $L_y = 3$ and $L_x = 9$. For comparison, the unit circle and approximating circles are also shown.

V. APPENDIX I: 1D LATTICE AND QUASI-1D LATTICE STRIPS

Our derivation of eq. (2.15) assumed that the lattice graph G has the property that removing a few edges does not cut it into disconnected parts. This property does not hold for a 1D lattice or quasi-1D lattice strips of sufficiently small width. Here we comment briefly on this. We consider first a one-dimensional lattice (line graph) with free or periodic boundary conditions, labelled FBC and PBC, respectively. We denote such graphs with n vertices as $L_{n,F}$ and $L_{n,P}$. The coordination number $\kappa = 2$ for $L_{n,P}$, and this is the effective value of the coordination number also for $L_{n,F}$ when $n \rightarrow \infty$, so that in both cases, $x_{1D} = v/q$. From elementary calculations one has the exact results

$$Z(L_{n,F}, q, v) = q^n (1 + x_{1D})^{n-1} \quad (5.1)$$

and

$$Z(L_{n,P}, q, v) = q^n [(1 + x_{1D})^n + (q-1)x_{1D}^n] \quad (5.2)$$

As in the text, we focus on large n and large q . Aside from the zero at $q = 0$, which is not relevant in this case, the zeros of $Z(L_{n,F}, q, v)$ occur at the single point

$$x_{1D} = -1 \quad (FBC) . \quad (5.3)$$

Note that the number of edges for this graph is $e(L_{n,F}) = n - 1$. Because the degree in q of the coefficient $c_j(q)$ defined in eq. (2.1) is $p_j = n - j$, all terms have the same order and none can be neglected.

In the limit $n \rightarrow \infty$, followed by $q \rightarrow \infty$, the zeros of $Z(L_{n,P}, q, v)$ are given by the solution to the equation $|1 + x_{1D}| = |x_{1D}|$, which is the vertical line $Re(x_{1D}) = -1/2$ in the x_{1D} plane, i.e.,

$$x_{1D} = -\frac{1}{2} + iy \quad (PBC) . \quad (5.4)$$

where $-\infty \leq y \leq \infty$. As these exact results show, the 1D case is different from the thermodynamic limit of lattices with dimensionality $d \geq 2$ in that the locus of zeros is strongly dependent upon the choice of boundary conditions and, moreover, is not the circle $|x_\Lambda| = 1$.

In contrast, for strips of the square lattice with various types of boundary conditions that maintain the duality of the infinite square lattice, we have shown via exact solutions in Ref. [22] that as $q \rightarrow \infty$, the zeros do lie exactly on the unit circle $|x_\Lambda| = 1$. For these strips we also found that for large but finite q , the locus \mathcal{B} consists of the union of (i) a self-conjugate portion of this unit circle given by $x_{sq} = e^{i\theta}$ with $\theta_0 \leq \theta \leq \pi$ and $-\pi \leq \theta \leq -\theta_0$ (where the angle θ_0 depends on the strip) with (ii) a line segment $-\rho \leq x_{sq} \leq -1/\rho$ on the negative real axis, where $\rho > 1$ is a positive real constant (see the plots given in Ref. [22]). The arc of the unit circle and the line segment intersect at $x_{sq} = -1$. As $q \rightarrow \infty$, $\rho \rightarrow 1$ and $\theta_0 \rightarrow 0$. Thus, for large but finite q , \mathcal{B} is almost the unit circle except for a small line segment centered at $x_{sq} = -1$ and a gap in the circle in the vicinity of $x_{sq} = 1$. As we discussed in Ref. [22], these deviations can be understood from the fact that the large- q expansion of the dominant eigenvalues of the transfer matrix contain poles at $x_{sq} = \pm 1$, showing that regardless of how large q is, the large- q expansion breaks down at these two points.

More generally, we have carried out similar large- q expansions for the dominant eigenvalues of the transfer matrix for quasi-one-dimensional strips of several lattices with different boundary conditions. We find that for the strips we have considered, these expansions exhibit singularities on the unit circle $x_\Lambda = 1$ for strips with periodic transverse boundary conditions but not for strips with free transverse boundary conditions. For example, we find that this expansion for the $L_y = 2$ cylindrical strip of the square lattice has branch-point singularities at $x_{sq} = \pm e^{i\pi/6}$ and $x_{sq} = \pm e^{-i\pi/6}$. Similarly, for the $L_y = 2$ cylindrical strip of the triangular lattice we find that the large- q expansion of the dominant eigenvalues has branch-point singularities at $x_{tri} = \pm 1$, $x_{tri} = \pm e^{i\pi/3}$, and $x_{tri} = \pm e^{-i\pi/3}$.

These deviations are characteristic of certain quasi-one-dimensional strips, which do not satisfy the premises of our general analytic results in Section II. We do not find such deviations for the thermodynamic limits of sections of regular lattices of dimensionality $d \geq 2$ in the limit of large q .

[1] F. Y. Wu, Rev. Mod. Phys. **54** (1982) 235.

[2] R. J. Baxter, *Exactly Solved Models* (Academic Press, New York, 1982).

[3] P. Pearce and R. B. Griffiths, J. Math. Phys. A **13**, 2143 (1980).

[4] J. Glazier, M. Anderson, and G. Grest, Philos. Mag. B **62**, 615 (1990); Y. Jiang and J. Glazier, Philos. Mag. Lett. **74**, 119 (1996).

[5] P. W. Kasteleyn and C. M. Fortuin, J. Phys. Soc. Jpn. **26** (Suppl.), 11 (1969); C. M. Fortuin and P. W. Kasteleyn,

Physica **57**, 536 (1972).

[6] M. E. Fisher, *Lectures in Theoretical Physics* (Univ. of Colorado Press, 1965), vol. 7C, p. 1.

[7] R. Abe, T. Dotera, and T. Ogawa, Prog. Theor. Phys. **85**, 509 (1991).

[8] V. Matveev and R. Shrock, J. Phys. A **28**, 5235 (1995).

[9] P. Martin and J. M. Maillard, J. Phys. A **19**, L547 (1986).

[10] P. P. Martin, *Potts Models and Related Problems in Statistical Mechanics* (World Scientific, Singapore, 1991).

[11] C. N. Chen, C. K. Hu, and F. Y. Wu, Phys. Rev. Lett.

- 76**, 169 (1996).
- [12] F. Y. Wu, G. Rollet, H. Y. Huang, J. M. Maillard, C. K. Hu, and C. N. Chen, Phys. Rev. Lett. **76**, 173 (1996).
- [13] V. Matveev and R. Shrock, Phys. Rev. **E54**, (1996) 6174.
- [14] H. Feldmann, R. Shrock, and S.-H. Tsai, Phys. Rev. E **57**, 1335 (1998),
- [15] H. Feldmann, A. J. Guttmann, I. Jensen, R. Shrock, and S.-H. Tsai, J. Phys. A **31**, 2287 (1998).
- [16] H. Kluepfel and R. Shrock, unpublished; H. Kluepfel, Stony Brook thesis “The q -State Potts Model: Partition Functions and Their Zeros in the Complex Temperature and q Planes” (July, 1999).
- [17] S.-Y. Kim and R. Creswick, Phys. Rev. **E63**, 066107 (2001).
- [18] R. Shrock, Physica A **283**, 388 (2000).
- [19] S.-C. Chang and R. Shrock, Physica A **286**, 189 (2000).
- [20] S.-C. Chang and R. Shrock, Physica A **296**, 183 (2001).
- [21] S.-C. Chang and R. Shrock, Physica A **296**, 234 (2001).
- [22] S.-C. Chang and R. Shrock, Phys. Rev. E **64**, 066116 (2001).
- [23] S.-C. Chang, J. Salas, and R. Shrock, J. Stat. Phys. **107** 1207 (2002).
- [24] F. Y. Wu, J. Mathematical and Computer Modelling **26**, 269 (1997).
- [25] H. Y. Huang and F. Y. Wu, Int. J. Mod. Phys. B **11**, 121 (1997).
- [26] L. Mittag and M. Stephen, J. Phys. A **7**, L109 (1974).